

# Rationale for the Acidity of Meldrum's Acid. Consistent Relation of C–H Acidities to the Properties of Localized Reactive Orbital

Satoshi Nakamura, Hajime Hirao,<sup>†</sup> and Tomohiko Ohwada\*

Graduate School of Pharmaceutical Sciences, The University of Tokyo, 7-3-1 Hongo, Bunkyo-ku, Tokyo 113-0033, Japan

ohwada@mol.f.u-tokyo.ac.jp

Received April 2, 2004

Detailed investigation on the origin of the acidity of the  $\alpha$ -protons of a set of the carbonyl molecules was carried out on the basis of properties of the localized molecular orbital. An anomalously high acidity of Meldrum's acid, as compared with those of dimedone and dimethyl malonate, is one of the well-known but unresolved issues. The well-localized  $\sigma$  orbitals of the C–H bonds at the  $\alpha$ -position of the carbonyl groups can be obtained with the reactive hybrid orbital (RHO) theory. We found that the energy levels of the unoccupied RHOs of the C–H moiety of Meldrum's acid and other carbonyl compounds showed a good linear correlation with the experimental deprotonation energies. This is probably because the deprotonation reaction to form the proposed naked anions in a polar solvent is a highly endothermic process, in which the thermodynamic energy differences between the neutral molecules and the corresponding anions approximately coincide with the activation energies. We also investigated the effect of the conformational change upon deprotonation on the electron-accepting energy level of the relevant C–H bonds of cyclic/acyclic and monocarbonyl/dicarbonyl compounds. A conformational change occurs in the cases of cyclic six-membered compounds, but its influence on the reactivity of the C–H bond is small. The acidity of dicarbonyl compounds, including Meldrum's acid, showed a good correlation with the deviations from the perpendicular position of the dihedral angles of the relevant C–H bond with respect to the adjacent carbonyl C=O bond. This angle parameter can be related to the magnitude of the in-phase orbital interaction between the  $\sigma^*_{\text{CH}}$  and  $\pi^*_{\text{C=O}}$  orbitals, which facilitate electron acceptance. These results indicated that the acidity of the  $\alpha$ -proton of carbonyl compounds can be represented in terms of the electron-accepting orbital levels of the unoccupied RHO of the C–H moiety. All the linear relationships found in the present work strongly suggested that the acidity of Meldrum's acid, which is conventionally regarded as an anomaly, is consistent with those of the other carbonyl compounds.

## Introduction

Understanding the origin of the acidity of C–H acids, particularly that of  $\alpha$ -protons of a carbonyl group, is a significant challenge in physical organic chemistry. One of the well-known but unsettled issues is the anomalously high acidity of Meldrum's acid (**1**, Figure 1;  $\text{p}K_{\text{a}}$  7.3, in DMSO at 25 °C).<sup>1</sup> Meldrum's acid is significantly more acidic than dimedone, a diketone analogue (**5**,  $\text{p}K_{\text{a}}$  11.2, in DMSO at 25 °C),<sup>1</sup> and dimethyl malonate, an open-chain analogue of Meldrum's acid (**7**,  $\text{p}K_{\text{a}}$  15.9, in DMSO at 25 °C).<sup>1</sup>

Much work has been done on this phenomenon. In one of the earliest studies, Arnett et al. attributed the anomalous acidity of Meldrum's acid to the geometrical constraint of (*E*)-conformation of the two ester groups, which is not seen in less acidic, large-ring-sized bislactones or open-chain diesters.<sup>2</sup> In Meldrum's acid, they

proposed that the enforced six-membered cyclic conformation restricts flexible rotation of the ester moiety, preventing conjugative stabilization of the ester carbonyl group and also increasing the electronegative electron-withdrawing effect of the unconjugated ether oxygens in the enforced (*E*)-conformation.

Ab initio molecular orbital calculations have also been applied to this issue.<sup>3–6</sup> Houk et al. discussed the energy differences between the esters in the two conformations ((*E*) and (*Z*)).<sup>3</sup> They found that there was great destabilization in the (*E*)-conformation of methyl acetate due to dipole–dipole repulsion between the ether oxygen atom and the carbonyl group, although such interaction was absent in the (*Z*)-conformer. They also found a significant reduction of the energy difference between the (*E*)- and

<sup>†</sup> Present address: Novartis Tsukuba Research Institute, 8 Ohkubo, Tsukuba, Ibaraki 300-2611, Japan.

(1) Arnett, E. M.; Maroldo, S. L.; Schilling, S. L.; Harrelson, J. A., Jr. *J. Am. Chem. Soc.* **1984**, *106*, 6759–6767.

(2) Arnett, E. M.; Harrelson, J. A., Jr. *J. Am. Chem. Soc.* **1987**, *109*, 809–812.

(3) Wang, X.; Houk, K. N. *J. Am. Chem. Soc.* **1988**, *110*, 1870–1872.

(4) Wiberg, K. B.; Laidig, K. E. *J. Am. Chem. Soc.* **1988**, *110*, 1872–1874.

(5) Byun, K.; Mo, Y.; Gao, J. *J. Am. Chem. Soc.* **2001**, *123*, 3974–3979.

(6) Lee, I.; Ham, I. S.; Kim, C. K.; Lee, H. W. *Bull. Korean Chem. Soc.* **2003**, *24*, 1141–1149.

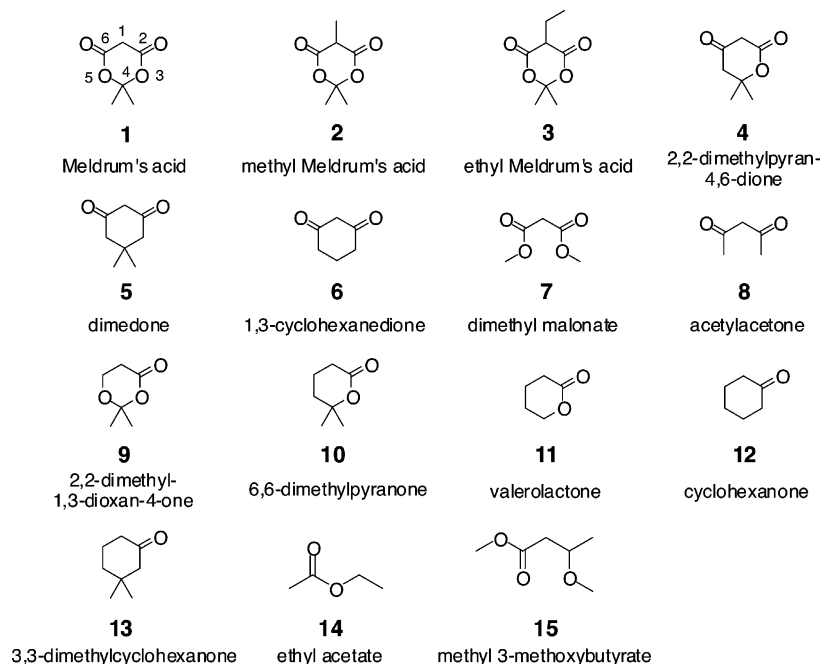


**FIGURE 1.** Relevant carbonyl compounds.

(*Z*)-conformers upon the formation of the corresponding enolate anions, though the (*Z*)-enolate anion of methyl acetate was still more stable than the (*E*)-enolate anion. Thus, these authors postulated that the ester in the (*E*)-conformation should be essentially more acidic than that in the (*Z*)-conformation, and this was consistent with the (*E*)-conformation structure of Meldrum's acid. This study partially accounted for the anomalous acidity of Meldrum's acid.

Wiberg et al. also calculated the deprotonation energies of the (*E*)- and (*Z*)-conformers of methyl acetate, and they found that the deprotonation energy from the (*E*)-conformer of the ester was smaller by 4.7 kcal/mol than that of the (*Z*)-conformer.<sup>4</sup> In the (*E*)-conformer of the acetate anion, the electrostatic attraction between the negatively charged methine moiety and the partially positively charged methyl group of the methoxy group stabilized the whole molecule.

More recently, Gao et al. pointed out that there was a significant stabilizing effect on the enolate anion due to the anomeric effect, which is characteristic of Meldrum's acid.<sup>5</sup> This effect stems from the structural features of the enolate anion of Meldrum's acid, i.e., the anomeric effect between the oxygen lone pair electrons of the ether oxygen atom (O5) and the vacant antibonding  $\sigma^*$  orbital of the O3 (the ether)–C4 bond (See Figure 1, 1). This type of stabilization is unavailable in the neutral Meldrum's acid. They also studied the solvent effect on the stability of the neutral and the anionic enolate forms of Meldrum's acid by using combined QM/MM Monte Carlo simulations. Lee et al. also attributed the origin of the anomalously high acidity of Meldrum's acid to specific increase of electron-delocalization of the nonbonding electrons of the carbanion moiety to the juxtaposed vacant carbonyl  $\pi^*$  orbitals and 1,4-attractive electrostatic interactions (between C<sub>1</sub> and C<sub>4</sub>) upon deprotonation.<sup>6</sup>

All of the previous studies, by focusing on stabilizing or destabilizing interactions specific to Meldrum's acid and its conjugate base, have been able to rationalize the anomalous acidity of Meldrum's acid, at least in part. However, there have been few studies to evaluate the nature of the molecular orbitals of a large set of the neutral carbonyl molecules and the anions, which would be both relevant to the C–H acidity.<sup>6</sup> Here we evaluate the acidities of the C–H bonds of Meldrum's acid and related carbonyl compounds in terms of the electron-accepting ability of the relevant  $\sigma_{\text{CH}}^*$  orbitals, based on evaluation of the energy levels of reactive localized orbitals, obtained by applying the reactive hybrid orbital (RHO) theory.<sup>7</sup> We found the significant correlation between the deprotonation energies and the orbital energy levels of the unoccupied RHOs of the  $\alpha$ -C–H bonds.

## Computational Methods

Geometry optimizations were performed with density functional theory (DFT) calculations at the B3LYP/6-311+G\*\* (5d) level using a suite of Gaussian 98 programs.<sup>8</sup> Vibration frequency analyses were also performed at the same level to establish whether the obtained structures corresponded to energy minima or saddle points on the potential energy surfaces. The energy levels of the canonical and the localized

(7) Hirao, H.; Ohwada, T. *J. Phys. Chem. A* **2003**, *107*, 2875–2881.

(8) Frisch, M. J.; Trucks, G. W.; Schlegel, H. B.; Scuseria, G. E.; Robb, M. A.; Cheeseman, J. R.; Zakrzewski, V. G.; Montgomery, J. A.; Stratmann, R. E.; Burant, J. C.; Dapprich, S.; Millam, J. M.; Daniels, A. D.; Kudin, K. N.; Strain, M. C.; Farkas, O.; Tomasi, J.; Barone, V.; Cossi, M.; Cammi, R.; Mennucci, B.; Pomelli, C.; Adamo, C.; Clifford, S.; Ochterski, J.; Petersson, G. A.; Ayala, P. Y.; Cui, Q.; Morokuma, K.; Malick, D. K.; Rabuck, A. D.; Raghavachari, K.; Foresman, J. B.; Cioslowski, J.; Ortiz, J. V.; Stefanov, B. B.; Liu, G.; Liashenko, A.; Piskorz, P.; Komaromi, I.; Gomperts, R.; Martin, R. L.; Fox, D. J.; Keith, T. A.; Al-Laham, M. A.; Peng, C. Y.; Nanayakkara, A.; Gonzalez, C.; Challacombe, M.; Gill, P. M. W.; Johnson, B. G.; Chen, W.; Wong, M. W.; Andres, J. L.; Head-Gordon, M.; Replogle, E. S.; Pople, J. A. *Gaussian 98*; Gaussian, Inc.: Pittsburgh, PA, 1998.

**TABLE 1.** Deprotonation Parameters of Relevant Carbonyl Compounds

| compound                 | solution phase  |   | gas phase                             |                            |
|--------------------------|-----------------|---|---------------------------------------|----------------------------|
|                          | $pK_{a,DMSO}^b$ | $\Delta G_{i,DMSO}^{\circ}$ (kcal/mol) <sup>b</sup> | $\Delta G_{i,gas}^{\circ}$ (kcal/mol) | PA (kcal/mol) <sup>f</sup> |
| <b>1</b>                 | 7.32            | 11.6  |                                       | 328.4                      |
| <b>2-a</b> <sup>a</sup>  | 7.42            | 11.7  |                                       | 328.8                      |
| <b>3-a</b> <sup>a</sup>  | 7.57            | 11.9  |                                       | 327.4                      |
| <b>4</b>                 | 10.5            | 15.9  |                                       | 331.4                      |
| <b>5</b>                 | 11.2            | 16.9  | 338.9 <sup>c</sup>                    | 333.1                      |
| <b>6</b>                 | 10.3            | 15.6  |                                       | 333.3                      |
| <b>7</b>                 | 15.9            | 23.2  |                                       | 344.5                      |
| <b>8</b>                 | 13.3            | 19.7  | 343.7 <sup>c</sup>                    | 338.3                      |
| <b>9</b>                 | 23.3            | 33.3  |                                       | 361.9                      |
| <b>10</b>                | 24.5            | 34.9  |                                       | 366.4                      |
| <b>11</b>                | 25.2            | 36.0  | 358.4 <sup>d</sup>                    | 366.0                      |
| <b>12</b>                | 26.3            | 37.4  | 358.7 <sup>e</sup>                    | 367.8                      |
| <b>13</b>                | 25.8            | 36.8  |                                       | 366.3                      |
| <b>14-a</b> <sup>a</sup> | 27.5            | 39.0  |                                       | 372.1                      |
| <b>15-b</b> <sup>a</sup> | 26.5            | 37.8  |                                       | 365.5                      |

<sup>a</sup> The most stable conformer of the molecule is used. <sup>b</sup>  $pK_a$  values in DMSO at 25°C were cited from ref 2. <sup>c</sup> Reference 24. <sup>d</sup> Reference 25. <sup>e</sup> Reference 26. <sup>f</sup> All factors were calculated at the B3LYP/6-311+G\*\* (5d) level. Proton affinity (PA) of the conjugated base is defined as  $PA = -\Delta H_{298} = -\Delta E_0 - \Delta ZPE + 5/2RT$ .  $\Delta E_0$  is difference of the total energy at 0 K between a carbonyl molecule and its corresponding enolate anion.  $\Delta ZPE$  is the difference of zero-point energy between an acid and its conjugate base, which is scaled by the factor of 0.963.  $R$  is the gas constant.  $T$  is temperature (here 298.15 K).

orbitals of the compounds discussed below were calculated at the RHF/6-31G\* (5d) level on the basis of the B3LYP/6-311+G\*\* (5d) optimized structures. Orbital representations were created with MOLEKEL 4.2, using a contour value of 0.05. <sup>9</sup>

## Results and Discussion

**Coincidence of Experimental Solution Acidity and Calculated Gas-Phase Acidity.** We optimized the structures of the carbonyl compounds **1–15** (Supporting Information Figure S1).<sup>2</sup> The energetic and structural parameters are shown in Table 1. Some compounds have several stable conformations, and we compared the relative energies of these conformers (Table 1 and Supporting Information Figure S1). We also optimized the deprotonated species (anions) of these carbonyl molecules **1–15** (see Supporting Information). Meldrum's acid **1** has two unequivalent hydrogen atoms at the  $\alpha$ -position of the two carbonyl groups, but the calculated structures of the two corresponding anions become identical after optimization, whichever proton is removed. Similarly, several possible structures of the corresponding anions of other compounds, which can be formed by removal of one of the protons at the  $\alpha$ -position of the carbonyl group, turned out to converge after structural optimization.

The conformations of Meldrum's acid **1** and its related six-membered heterocyclic compounds, such as **2** and **3**, are boatlike, whereas those of the carbocyclic dicarbonyl compounds, such as dimedone **5**, are chairlike. These structural features are consistent with the previous study by Arnett.<sup>2</sup> This diversity would stem from the different stereoelectronic effects of the ether oxygen atoms.<sup>6,10</sup>

(9) Flükiger, P.; Lüthi, H. P.; Portmann, S.; Weber, J. *MOLEKEL* 4.2; Swiss Center for Scientific Computing: Manno, Switzerland, 2000–2002.

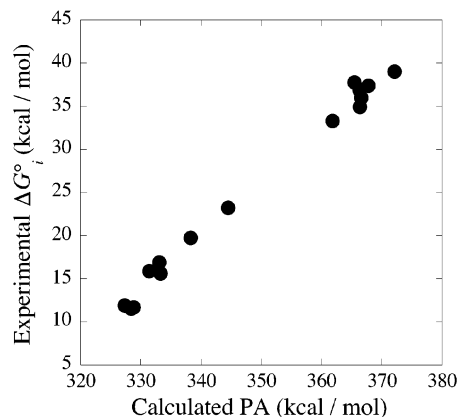


**FIGURE 2.** Correlation between proton affinity and standard ionization energy. Proton affinity (PA) was defined as  $PA = -\Delta H_{298} = -\Delta E_0 - \Delta ZPE + 5/2RT$ .  $\Delta ZPE$  was scaled by the factor 0.963. Standard ionization energy ( $\Delta G_i^{\circ}$ ) was defined as eq 1.  $T = 298.15$  K. The PA values were calculated at the B3LYP/6-311+G\*\* (5d) level.

Generally the acidities in solution are greatly different from those in the gas phase because of the solvent effect. However, it has been established that the acidities of C–H acids in a polar aprotic solvent, such as DMSO, correspond well to those in the gas phase.<sup>11</sup> A naked anion was proposed to be formed in this solvent, which is relevant to the gas phase state. The acidity constants of the carbonyl compounds **1–15** in DMSO at 25 °C have been reported (Table 1).<sup>2</sup> The experimental standard ionization energies ( $\Delta G_i^{\circ}$ ) were calculated on the basis of the  $pK_a$  values in DMSO, using the reported formula<sup>2</sup>

$$\Delta G_i^{\circ} = 2.303RT(pK_a + \log 14) \quad (1)$$

These  $\Delta G_i^{\circ}$  values are shown in Table 1. The proton affinity (PA) of the conjugate base, i.e., the change of the standard enthalpies between the neutral carbonyl molecule and its enolate anion, is the gas-phase acidity, which can be evaluated by calculation. We used DFT calculations at the B3LYP/6-311+G\*\* (5d) level to evaluate the total energies of molecules. These energies were corrected with scaled zero-point energy (ZPE) and thermal correction at 298.15 K (Table 1). These two kinds of energy changes upon deprotonation, that is, the experimental  $\Delta G_i^{\circ}$  and the calculated PA, showed an excellent correlation ( $r = 0.996$ , Figure 2). This result allowed us to investigate the relationships between the parameters obtained in the calculations (i.e., in the gas phase) and the deprotonation energies of the compounds (in solution).

**Intrinsic Electron-Accepting Ability of the C–H Bond, Represented by the Reactive Hybrid Orbital (RHO).** Although the frontier orbital (FO) theory is generally accepted as one of the most effective methods to explain the reactivity of a molecule,<sup>12</sup> the validity of

(10) Deslongchamps, P. *Stereoelectronic Effects in Organic Chemistry*; Pergamon Press: New York, 1983.

(11) (a) Hehre, W. J.; Radom, L.; Schleyer, P. v. R.; Pople, J. A. *Ab Initio Molecular Orbital Theory*; Wiley-Interscience: New York, 1986; pp 411–413. (b) Bordwell, F. G. *Pure Appl. Chem.* **1977**, *49*, 963–968. (c) Bordwell, F. G. *Acc. Chem. Res.* **1988**, *21*, 456–463.

(12) Fukui, K.; Yonezawa, T.; Shingu, H. *J. Chem. Phys.* **1952**, *20*, 722–733.

the parameters derived from the FO theory becomes uncertain as the size of the molecule increases. This is partially because the frontier orbitals are canonical molecular orbitals, which can spread over the whole molecule. Consequently, these specified orbitals do not always represent the reaction center of the molecule. Although several localized molecular orbital (LMO) methods such as the Rudenberg, Boys, Mezey, and NLMO methods have been well established,<sup>13</sup> it is still difficult to access an orbital that directly reflects molecular reactivity. Recently, an a priori method to represent the reactive localized orbital was proposed, which was called the reactive hybrid orbital (RHO) method.<sup>7</sup> Using this method, we can obtain an approximate reactive orbital of a molecule in an organic reaction. It would be a powerful method to evaluate the reactivity of a molecule and the origin of it, especially to compare them between similar molecules. Cleavage of an acidic C–H bond can be regarded as a result of electron delocalization of a base into the antibonding orbital of the relevant C–H bond. In this work, we evaluated the electron-accepting orbital levels of the C–H bonds of the carbonyl compounds with the RHO method and examined the origin of the acidity of Meldrum's acid.

When an unoccupied orbital  $\phi_{\text{unoc}}$  is represented by a linear combination of canonical unoccupied MOs  $\psi_j$  as

$$\phi_{\text{unoc}} = \frac{\sum_j^{\text{unoc}} d_j \psi_j}{(\sum_j^{\text{unoc}} d_j^2)^{1/2}} \quad (2)$$

the energy level of the orbital  $\phi_{\text{unoc}}$  can be defined by  $\lambda_{\text{unoc}}$  as

$$\lambda_{\text{unoc}} = \frac{\sum_j^{\text{unoc}} d_j^2 \epsilon_j}{\sum_j^{\text{unoc}} d_j^2} \quad (3)$$

where  $\epsilon_j$  is the energy level of the canonical MO  $\psi_j$ , obtained by solving a Hartree–Fock–Roothaan equation. On the other hand, the orbital  $\phi_{\text{unoc}}$  can be represented in terms of a linear combination of atomic orbitals  $\chi_\mu$  as

$$\phi_{\text{unoc}} = \sum_\mu c_\mu \chi_\mu \quad (4)$$

If we extract only the terms containing the AOs on the atoms of the electrophilic center (in this work, we defined the hydrogen and carbon atoms of the  $\alpha$ -position of the relevant carbonyl groups as the reaction center, and they are denoted here by  $A$ ) from eq 5

$$\phi'_{\text{unoc}} = \sum_{\mu \in A} c_\mu \chi_\mu \quad (5)$$

we can define functions  $f_{\text{unoc}}$  and  $\rho_{\text{unoc}}$ , respectively:

$$f_{\text{unoc}} = \langle \phi_{\text{unoc}} | \phi'_{\text{unoc}} \rangle \quad (6)$$

$$\rho_{\text{unoc}} = f_{\text{unoc}} / \lambda_{\text{unoc}} \quad (7)$$

The function  $f_{\text{unoc}}$  represents the number of electrons that can be accepted from an electron donor. Then, the function  $\rho_{\text{unoc}}$  is a balance of localization and the energy level of an unoccupied orbital. We obtained a distinctive set of  $d_j$  values in eq 2, from which the maximum value of  $\rho_{\text{unoc}}$  can be obtained by minimizing  $1/\rho_{\text{unoc}}$  numerically with the Davidson–Fletcher–Powell method.<sup>14</sup> The orbital  $\phi_{\text{unoc}}$ , represented by eq 2 with the optimized  $d_j$  values, is specifically called the unoccupied RHO here. The relative electron-accepting level of the electrophilic center can be evaluated by  $\lambda_{\text{unoc}}$ , the energy level of the unoccupied RHO, or the factor  $\rho_{\text{unoc}}$ , a reactivity index of the unoccupied RHO. The smaller value of  $\lambda_{\text{unoc}}$  or the bigger value of  $\rho_{\text{unoc}}$  represent the higher electron-accepting level of the reaction center.

In this work, we defined the carbon and the hydrogen atoms of  $\alpha$ -position of a carbonyl group as the electrophilic center of a compound.

**Evaluation of Local Electron-Accepting Levels of the Relevant C–H Bond of Meldrum's Acid and Related Carbonyl Compounds. (A) Calculated Energy Levels of the Relevant Orbitals.** We calculated the local electron-accepting levels ( $\lambda_{\text{unoc}}$ ) of the C–H moiety at the  $\alpha$ -position of Meldrum's acid and related carbonyl compounds with the RHO method (Table 2). The energy levels of the LUMOs of the molecules are also shown in it. In most cases the  $\alpha$ -protons of the carbonyl compounds are nonequivalent. In the cases of the cyclic compounds, the  $\lambda_{\text{unoc}}$  values of the axial C–H bonds are lower in energy than those of the equatorial C–H bonds. In the cases of the acyclic compounds, one of the C–H bonds is superior to other bonds in terms of the electron-accepting level. This is consistent with the postulate that overlap of the C–H bond with the carbonyl  $\pi^*$  orbital modifies the electron-accepting level of the C–H bond; that is, the greater the overlap, the lower the electron-accepting level.<sup>15</sup>

The comparison of the  $\lambda_{\text{unoc}}$  values of **14-a** and **14-b** supports the previous postulate that the ester in the (*E*)-conformation is essentially more acidic than that in the (*Z*)-conformation.<sup>3</sup> That is, the  $\lambda_{\text{unoc}}$  value of **14-b** ((*E*)-conformer) was smaller than that of **14-a** ((*Z*)-conformer), which indicates that **14-b** is superior to **14-a** as an acid.

**(B) Orbital Component.** The LUMO of Meldrum's acid **1** is shown in Figure 3A. The LUMO is mainly composed of in-phase combination of the  $\sigma_{\text{CH}}^*$  orbital of the axial C–H bond and the adjacent carbonyl  $\pi^*$  orbital, together with a small contribution of the ether oxygen p-type orbital. The localizability onto the relevant  $\sigma_{\text{CH}}^*$  bond of the LUMO is apparently low. The unoccupied RHO of Meldrum's acid **1** is also shown in Figure 3B.<sup>16</sup> The orbital is well localized onto the carbon and the hydrogen atoms of the reaction center, and a contribution of the in-phase combination of the adjacent carbonyl  $\pi^*$

(14) (a) Fletcher, R.; Powell, M. J. D. *Comput. J.* **1963**, *6*, 163–168. (b) Reddy, P. J.; Zimmermann, H. J.; Hussain, A. J. *Comput. Appl. Math.* **1975**, *1*, 255–265.

(15) (a) Ohwada, T. *Tetrahedron* **1993**, *49*, 7649–7656. (b) Rosenberg, R. E.; Mohrig, J. R. *J. Am. Chem. Soc.* **1997**, *119*, 487–492.

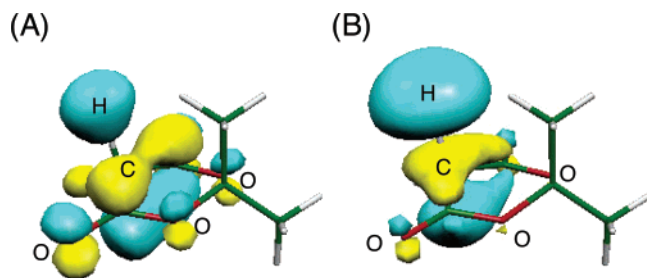
(13) Reed, A. E.; Weinhold, F. *J. Chem. Phys.* **1985**, *83*, 1736–1740.



**TABLE 2.** Calculated Energetic Values of LUMO and Unoccupied RHO of the Reaction Center of Relevant Carbonyl Compounds<sup>a</sup>

| compd       | $E_{\text{LUMO}}$<br>(kcal/mol) <sup>b</sup> | $\lambda_{\text{unoc}}$ (kcal/mol) <sup>c</sup> |                    | $f_{\text{unoc}}$<br>(au) <sup>d</sup> | $\rho_{\text{unoc}}$ <sup>d</sup> |
|-------------|--|---|--------------------|--|-----------------------------------|
|             |  | axial<br>H                                      | equa-<br>torial H  |  |                                   |
| <b>1</b>    | 88.4   | 127.6   | 156.7              | 0.9648                                 | 4.746                             |
| <b>2-a</b>  | 89.2   | 128.2   |                    | 0.9617                                 | 4.707                             |
| <b>2-b</b>  | 87.8   |   | 134.3              | 0.9675                                 | 4.519                             |
| <b>3-a</b>  | 89.8   | 126.9   |                    | 0.9594                                 | 4.744                             |
| <b>3-b</b>  | 86.8   |   | 132.4              | 0.9886                                 | 4.687                             |
| <b>4</b>    | 79.8   | 135.4   | 153.9              | 0.9747                                 | 4.518                             |
| <b>5</b>    | 78.8   | 138.2   | 184.8              | 0.9662                                 | 4.388                             |
| <b>6</b>    | 76.3   | 137.5   | 184.1              | 0.9583                                 | 4.373                             |
| <b>7</b>    | 110.4  | 164.6   | 168.4              | 1.0696                                 | 4.077                             |
| <b>8</b>    | 75.1   | 160.1   | 160.1              | 0.9986                                 | 3.915                             |
| <b>9</b>    | 110.3  | 162.4   | 175.2              | 1.0247                                 | 3.961                             |
| <b>10</b>   | 113.3  | 165.3   | 179.8              | 1.0265                                 | 3.897                             |
| <b>11</b>   | 110.2  | 163.3   | 178.0              | 1.0212                                 | 3.925                             |
| <b>12</b>   | 97.3   | 169.8   | 189.3              | 1.0157                                 | 3.754                             |
| <b>13</b>   | 98.2   | 169.8 <sup>e</sup>                              | 170.9 <sup>e</sup> | 1.0183                                 | 2.764                             |
| <b>14-a</b> | 119.0  | 178.8 <sup>f</sup>                              | 179.4 <sup>f</sup> | 1.0681                                 | 3.748                             |
| <b>14-b</b> | 118.7  | 166.8 <sup>f</sup>                              | 167.1 <sup>f</sup> | 1.0283                                 | 3.868                             |
| <b>15-a</b> | 116.2  | 172.9 <sup>f</sup>                              | 192.5 <sup>f</sup> | 1.0304                                 | 3.740                             |
| <b>15-b</b> | 119.5  | 172.1 <sup>f</sup>                              | 197.1 <sup>f</sup> | 1.0477                                 | 3.819                             |
| <b>15-c</b> | 114.6  | 176.4 <sup>f</sup>                              | 182.0 <sup>f</sup> | 1.0729                                 | 3.817                             |

<sup>a</sup> All values were calculated at the RHF/6-31G\* (5d)/B3LYP/6-311+G\*\* (5d) level. <sup>b</sup> The energy levels of LUMOs. <sup>c</sup> The energy levels of the unoccupied RHOs of the  $\alpha$ -C-H moieties of the carbonyl groups. <sup>d</sup> The values of unoccupied RHOs, which have the lowest values of  $\lambda_{\text{unoc}}$ . <sup>e</sup> The two former values of  $\lambda_{\text{unoc}}$  are those of the axial C-H moieties, and the latter two are those of the equatorial C-H moieties. <sup>f</sup> The energy levels of the  $\alpha$ -methyl (14) or  $\alpha$ -methylene (15) C-H moieties of the carbonyl groups.

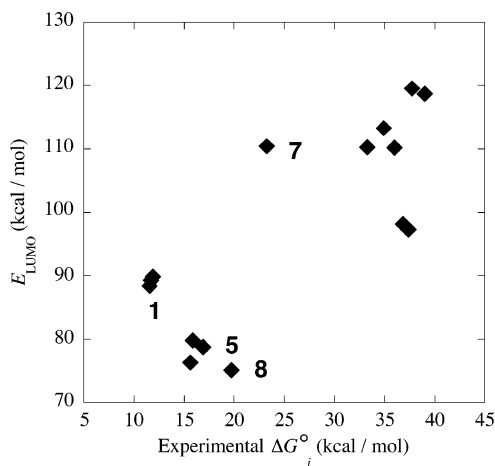
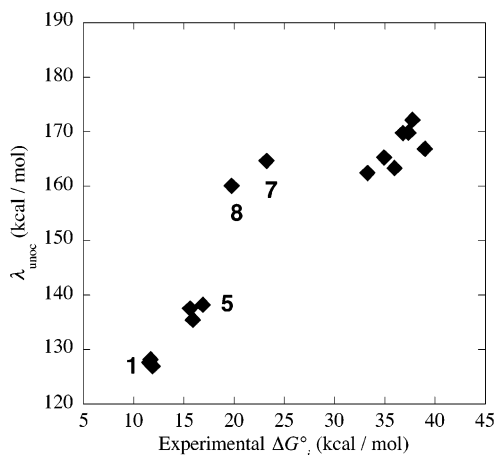
**FIGURE 3.** The unoccupied orbital pictures of Meldrum's acid **1** (RHF/6-31G\* (5d)/B3LYP/6-311+G\*\* (5d)). (A) LUMO of **1**. (B) Unoccupied RHO of reaction center of **1**.

orbitals can be seen. Here, the contribution of p-type orbitals of the ether oxygen atoms is minor.

**(C) Correlation between Orbital Energies and  $\Delta G_i$ .** We studied the relationship between the electron-accepting orbital levels of the relevant C-H bonds (the energy levels of the LUMO and RHO, respectively) and the experimentally determined deprotonation energy  $\Delta G_i$ . The energy level of the LUMOs is lower than that of RHOs because of delocalization. When the LUMO energy was plotted against  $\Delta G_i$ , the plot was scattered and there was no apparent correlation (Figure 4).<sup>17</sup>

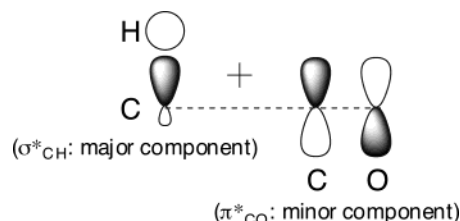
Next, we plotted the local electron-accepting levels  $\lambda_{\text{unoc}}$  of the RHO against experimental  $\Delta G_i$ . A better linear correlation was obtained (Figure 5), though the values of the acyclic dicarbonyl compounds **7** and **8** were slightly scattered.<sup>18–20</sup> The deviation observed in the cases of **7** and **8** is discussed later.

In the deprotonation process in a polar solvent, naked anions are proposed to be involved.<sup>11</sup> Because the depro-

**FIGURE 4.** Correlation between the experimental standard ionization energy ( $\Delta G_i^o$ ) and the calculated energy level of LUMO ( $E_{\text{LUMO}}$ ). The energies are calculated at the RHF/6-31G\* (5d)/B3LYP/6-311+G\*\* (5d) level.**FIGURE 5.** Correlation between the experimental standard ionization energy ( $\Delta G_i^o$ ) and calculated  $\lambda_{\text{unoc}}$  of the reaction center. The lowest values of  $\lambda_{\text{unoc}}$  were adopted for all of the compounds. The  $\lambda_{\text{unoc}}$  values were calculated at the RHF/6-31G\* (5d)/B3LYP/6-311+G\*\* (5d) level.

tonation reaction is significantly endothermic (Figure 6), the magnitudes of the proton affinity will coincide with those of the activation energies through a putative

(16) The major component of the unoccupied RHO is the  $\sigma^*_{\text{CH}}$  orbital. This result seems to be very reasonable. In a deprotonation reaction, a base attacks with its occupied orbital, such as a nitrogen lone pair of an amine, at the unoccupied orbital of a hydrogen atom. Since the  $\sigma^*_{\text{CH}}$  orbital is an antibonding orbital of carbon and hydrogen atomic orbitals, electron delocalization to the present orbital leads to C-H bond cleavage. Other remaining components also interact with the major component to influence the reactivity. Construction of the reactive orbital of deprotonation of carbonyl compounds:

(17) Regression coefficient of Figure 4:  $r = 0.783$ .

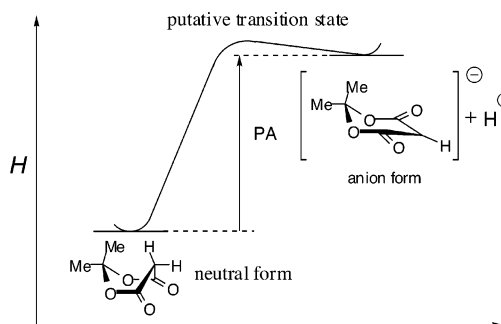


**FIGURE 6.** Energy profile of deprotonation of Meldrum's acid.

transition state of the proton removal, which is consistent with the Leffler–Hammond postulate. The occupied RHOs of the corresponding anions showed a much worse correlation with the experimental deprotonation energy  $\Delta G^\circ_i$  (Supporting Information). The superior correlation between the local electron-accepting levels ( $\lambda_{\text{unoc}}$ ) of the unoccupied RHOs of the C–H group and the experimental deprotonation energy  $\Delta G^\circ_i$  (Figure 5) suggested that an energy level of a RHO can reflect the orbital interaction around the transition state, particularly even at the late transition state. Apparently the LUMO is not a suitable descriptor in this process. We can also postulate that in the present case the feasibility of thermodynamic deprotonation approximately coincides with that of the C–H bond cleavage.

**Effects of Conformational Change upon Electron-Accepting Orbital Level of the C–H Bond.** To evaluate the conformational changes upon deprotonation, the transition structures of model deprotonation reactions of **1**, **5**, **6**, **7**, and **8** with LiH as a base were calculated at the B3LYP/6-311+G\*\* (5d) level (Figure 7).<sup>21</sup>

In the deprotonation transition structures, the dihedral angles of the C–H bond of interest with respect to the adjacent C=O bond were changed from those of the stable structures. We evaluated the changes of the sum of the absolute deviation of the dihedral angles from the perpendicular angle in the deprotonation transition structures.

Significantly reduced deviation was found in the cases of **7** and **8**. The changes of total deviation are  $-13.1^\circ$  and  $-50.4^\circ$ , respectively (see Figure 7). In the case of Meldrum's acid **1**, unexpectedly, the deviation in the transition structure is rather increased as compared with the stable conformation (the change of total deviation is  $+31.4^\circ$ ). In the cases of **5** and **6**, a very small change in total deviation takes place ( $+6.9^\circ$  and  $+4.2^\circ$ , respectively), while one of the carbonyl planes approaches the perpendicular to the relevant C–H bond. These results indicate that conformational changes upon deprotonation, particularly in the cases of the acyclic dicarbonyl compounds **7** and **8**, need to be considered. Thus, we calculated the  $\lambda_{\text{unoc}}$  values of **1**, **6**, **7**, and **8** for the optimized structures with fixation of the dihedral angles to those found in the deprotonation transition structures

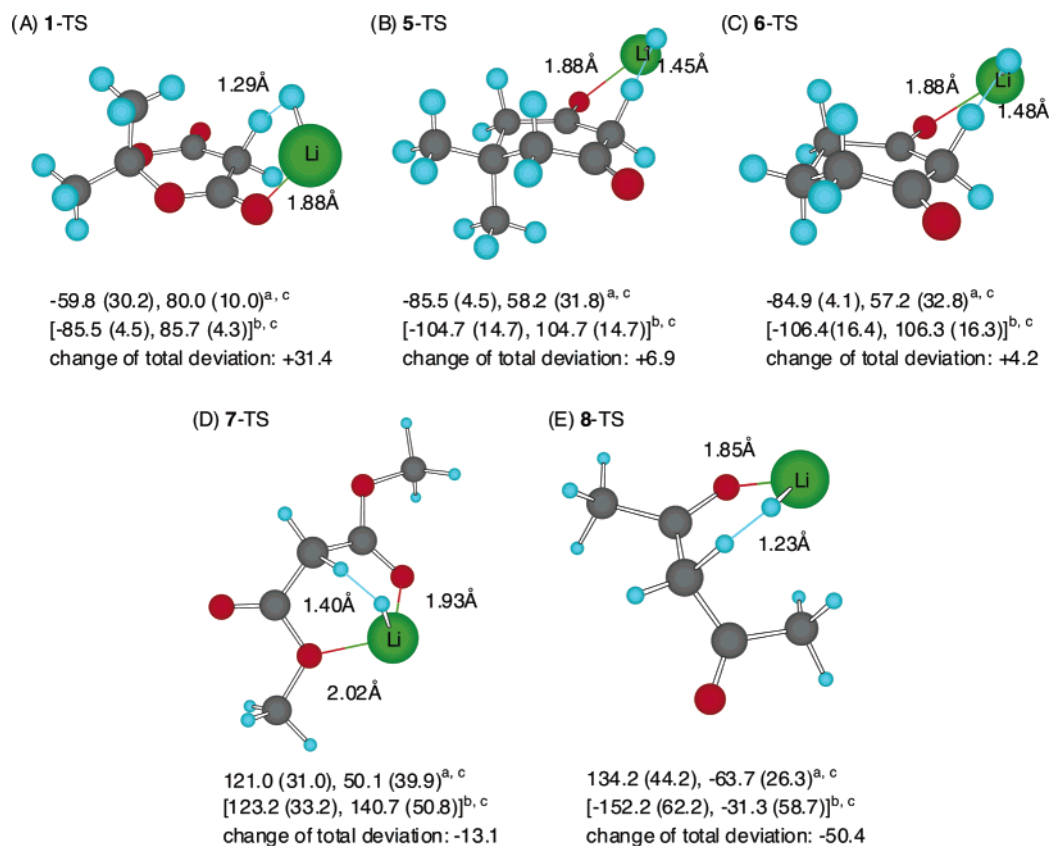


**FIGURE 7.** The transition structures for deprotonation reaction with LiH of (A) **1**, (B) **5**, (C) **6**, (D) **7**, and (E) **8**. A gray-colored sphere represents a carbon; blue, hydrogen; red, oxygen; green, lithium. All of the structures were obtained at the B3LYP/6-311+G\*\* (5d) level. <sup>a</sup>The dihedral angles of the transition structures. <sup>b</sup>The dihedral angles of the stable structures are given in brackets. <sup>c</sup>The deviation of the dihedral angles from the perpendicular angle are given in the parentheses.

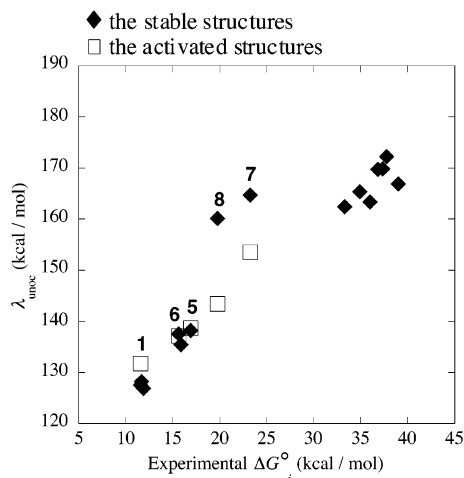


**FIGURE 8.** Correlation between the experimental standard ionization energy ( $\Delta G^\circ_i$ ) and  $\lambda_{\text{unoc}}$  values: (◆) the  $\lambda_{\text{unoc}}$  values of the stable structures; (□) the  $\lambda_{\text{unoc}}$  values of the activated structures. The  $\lambda_{\text{unoc}}$  values were calculated at the RHF/6-31G\* (5d)/B3LYP/6-311+G\*\* (5d) level.

as model transitional structures in DMSO (we call them the activated structures).<sup>22</sup>

As is clearly shown in Figure 8, the  $\lambda_{\text{unoc}}$  values of the acyclic systems **7** and **8** changed significantly in the activated structures from those based on the stable structures. On the other hand, the  $\lambda_{\text{unoc}}$  values of Meldrum's acid **1** and the cyclic dicarbonyl compounds **5** and **6** did not change significantly. With the use of these corrected  $\lambda_{\text{unoc}}$  values for **7** and **8** corresponding to those of the activated structures, a greatly improved correlation between the experimental  $\Delta G^\circ_i$  and the  $\lambda_{\text{unoc}}$  values was obtained (Figure 8).<sup>23–26</sup> This result indicates that there is a consistent relation between the C–H acidity of Meldrum's acid **1**, dimedone **5**, and dimethyl malonate **7** and the electron-accepting levels of the C–H bonds. Further, it was reported that long-chain cyclic carbonyl compounds (e.g., 1,5-dioxacycloheptadecane-2,4-dione (a 15-membered ring);  $pK_a$  15.14, 1,5-dioxacyclotridecane-2,4-dione (a 13-membered ring)  $pK_a$  15.22) show acidities almost equal to those of the acyclic carbonyl compounds.<sup>1</sup> This can be attributed to the flexibility of the dihedral angles between the C–H bonds and the adjacent carbonyl groups upon deprotonation, in a manner similar to that of the acyclic compounds.

**Origin of the Reactivity of Unoccupied RHO.** As shown in Figure 3B, the unoccupied RHO of Meldrum's acid is mainly composed of in-phase interaction between  $\sigma^*_{\text{CH}}$  and carbonyl  $\pi^*$  orbital. The electron-accepting levels  $\lambda_{\text{unoc}}$  of the C–H moiety can be related to the magnitude of overlap of the relevant  $\sigma^*_{\text{CH}}$  orbital and the

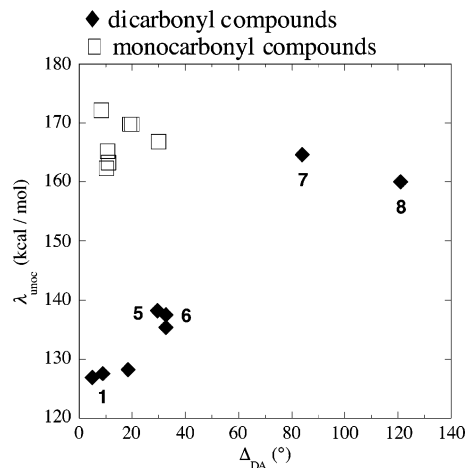


**FIGURE 9.** Correlation between the absolute value of the deviation of the dihedral angle between the C–H bond and the adjacent C=O bond from the perpendicular angle ( $\Delta_{\text{DA}}$ ) and the energy level of unoccupied RHO  $\lambda_{\text{unoc}}$ . The  $\lambda_{\text{unoc}}$  values of the stable structures were used: (◆) dicarbonyl compounds **1–8** (sum of  $\Delta_{\text{DA}}$  was used); (□) monocarbonyl compounds **9–15**.

adjacent carbonyl  $\pi^*$  orbital. We can represent this magnitude in terms of the absolute values of the deviation of the dihedral angles between the C–H bonds and the C=O bonds from the perpendicular angle (abbreviated here as  $\Delta_{\text{DA}}$ ). Thus, we plotted the  $\lambda_{\text{unoc}}$  values against  $\Delta_{\text{DA}}$  (Figure 9). The values of  $\lambda_{\text{unoc}}$  showed a good correlation with the summation of  $\Delta_{\text{DA}}$  in the cases of the dicarbonyl compounds **1–8**. In the case of dicarbonyl compounds, the C–H bond in the reaction center can interact with both of the adjacent carbonyl groups. On the other hand, C–H bond in a monocarbonyl compound can interact with only one carbonyl orbital fragment, which leads to the levels of  $\lambda_{\text{unoc}}$  higher than those of dicarbonyl compounds.

These results indicate that, despite the intervention of interaction with other fragments, the acidity of the C–H bond is strongly influenced by the arrangement of the relevant carbonyl group, particularly in the cases of dicarbonyl compounds.

## Conclusion

We applied here the RHO method, a newly proposed approach for construction of a reactive localized molecular

(18) Regression coefficient of Figure 5:  $r = 0.924$ . When the data for **7** and **8** are excluded, the regression coefficient increases:  $r = 0.993$ . Similarly when **7** and **8** are excluded in Figure 5, the regression coefficient is  $r = 0.835$ .

(19) On the basis of the orbital interaction theory,<sup>20</sup> the interaction energy  $\Delta E$  between the orbitals  $\varphi_i$  and  $\varphi_j$  is approximated as  $\Delta E \approx H_{ij}^2 / (E_i - E_j)$  where  $H_{ij}$  is the interaction Hamiltonian between  $\varphi_i$  and  $\varphi_j$ ,  $E_i$  and  $E_j$  are the  $\varphi_i$  and  $\varphi_j$  energies before interaction. Here we define  $C/\lambda_{\text{unoc}}$  as a reactivity standard. In the small range of  $\lambda_{\text{unoc}}$ ,  $C/\lambda_{\text{unoc}}$  should be approximately proportional to  $\lambda_{\text{unoc}}$ . So we plotted  $\lambda_{\text{unoc}}$  against  $\Delta G^\circ_i$ .

(20) Henri-Rousseau, O.; Texier, F. *J. Chem. Educ.* **1978**, *55*, 437–441.

(21) All the calculated transition structures involved coordination of the lithium cation to the oxygen atom of the carbonyl or ether group. In the case of dimethyl malonate **7**, only the Li-bidentate-type transition structure was found, whereas the monodentate-type structures were obtained in the cases of **1**, **5**, **6**, and **8**.

(22) Except for the dihedral angles, all the geometrical parameters were subject to optimization at the B3LYP/6-311+G\*\* (5d) level. The resultant structures were not different from the initial transition structures except for the length of the C–H bonds of the reaction center. (The C–H bonds of the transition structures were lengthened.) The  $\lambda_{\text{unoc}}$  values (kcal/mol) for the activated structures are as follows. (The values in the parentheses (kcal/mol) are the deviations of  $\lambda_{\text{unoc}}$  from the values of the stable structures.) **1**, 131.7 (+4.1); **5**, 138.7 (+0.5); **6**, 137.2 (–0.3); **7**, 153.5 (–11.1); **8**, 143.5 (–16.6).

(23) Regression coefficient of Figure 8:  $r = 0.987$ . (In the case of **7** and **8**,  $\lambda_{\text{unoc}}$  values of the activated structures were used.)

(24) Arnett, E. M.; Venkatasubramanian, K. G. *J. Org. Chem.* **1983**, *48*, 1569–1578.

(25) Karty, J. M.; Janaway, G. A.; Brauman, J. I. *J. Am. Chem. Soc.* **2002**, *124*, 5213–5221.

(26) Fu, Y.; Liu, L.; Li, R.; Liu, R.; Guo, Q. *J. Am. Chem. Soc.* **2004**, *126*, 814–822.

orbital, to the examination of the acidity of various carbonyl compounds. An excellent correlation between the experimental  $\Delta G^\circ_i$  and the local electron-accepting level of the unoccupied RHO ( $\lambda_{\text{unoc}}$ ) of the C–H moiety of the carbonyl compounds was found.

The conformational changes upon deprotonation were examined in some model TS structures (activated structures) of dicarbonyl compounds, and we found that the significant conformational change occurred in the cases of acyclic dicarbonyl molecules. Conformational change was also found in the cases of cyclic (six-membered) molecules, but the extent of the change and its influence on the reactivity of the C–H bond was relatively small. We also found that the acidity of the dicarbonyl compounds including Meldrum's acid showed a good correlation with the sum of the absolute deviations from the perpendicular positions of the dihedral angles of the relevant C–H bonds with respect to the adjacent carbonyl groups, which can be related to the magnitude of the in-phase orbital interaction between  $\sigma^*_{\text{CH}}$  and  $\pi^*_{\text{C=O}}$  orbitals. In the case of monocarbonyl compounds, however, there was no apparent correlation between  $\lambda_{\text{unoc}}$  and the dihedral angle. These results indicate that the acidity of the  $\alpha$ -proton of carbonyl compounds can be represented in terms of the electron-accepting level of a reactive localized C–H orbital, which can be modified by a strong intramolecular orbital interaction.

All of the linear relationships found in the present study strongly suggest that the high acidity of Meldrum's acid **1**, which is conventionally regarded as an anomaly, is consistent with those of other carbonyl compounds **2–15**.

**Acknowledgment.** This work was supported in part by a Grant-in-Aid from the Ministry of Education, Science, Sports, Culture and Technology, Japan, Uehara Memorial Foundation (to T.O.), and the Sumitomo Foundation (to T.O.). This work was partially supported by the Grant-in-Aid for Japan Society for the Promotion of Science (JSPS) Research Fellows (to S.N.). Some of the calculations were carried out at the Computer Center, the Institute for Molecular Science, and the Computer Center of the University of Tokyo. We thank these computational facilities for generous allotments of computer time.

**Note Added after ASAP Posting.** There was an error in eq 4 in the version posted ASAP on May 21, 2004; the corrected version was posted May 25, 2004.

**Supporting Information Available:** Calculated structural values, stable conformations of the relevant carbonyl compounds, Cartesian coordinates, number of imaginary frequencies, total energies of calculated species, and zero-point energies; data of occupied orbitals of anions. This material is available free of charge via the Internet at <http://pubs.acs.org>.

JO049456F